MRS Advances © 2019 Materials Research Society
DOI: 10.1557/adv.2019.52

Mechanical properties of polydopamine (PDA) thin films

Haoqi Li, Jiaxin Xi, Yao Zhao, Fei Ren

Department of Mechanical Engineering, College of Engineering, Temple University, Philadelphia, PA 19122, U.S.A.

ABSTRACT

Polydopamine (PDA) is a biopolymer, which can form uniform thin films on almost all solid substrates as well as at the liquid/air interface. Carbonized polydopamine possesses graphite-like structure and exhibits high electrical conductivity, which makes it a potential carbon-based thin film conductor. However, studies on mechanical behavior of PDA and its derived materials are very limited. In this study, PDA samples were synthesized through self-assembly of dopamine in aqueous solution. Elastic modulus of thin films was measured using the nanoindentation technique. It is shown that the Young's modulus of PDA thin film increased with increasing heat treatment temperature (up to 600˚C). Doping with Cu ions also increased the Young's modulus of PDA. Furthermore, all PDA thin films, with and without Cu, exhibited creep behavior.

INTRODUCTION

Polydopamine (PDA) is a biopolymer inspired by mussel chemistry [1]. It has attracted much attention owing to its interesting properties and ease of synthesis. An auto-oxidation process under mild conditions in dopamine solution [2] can yield nanoscale PDA powder with controllable size [3], smooth, crack-free, and thin coatings on solid substrates, or free-standing films at the solution/air interface [4]. Multiple function groups give PDA the ability to interact with other molecules and metal ions through secondary bonding or coordination bonding [5]. PDA is proposed to be used in surface modification with tailored hydrophobicity, target drug delivery, and capture of heavy metal ions for water treatment [6-9]. In addition, thin PDA films can also be converted to a graphite-like phase via heat treatment under protective atmosphere. Carbonized PDA (cPDA) is found to have an electrical conductivity [10] as high as 1.2 x 10^5 S/m which is comparable to reduced graphene oxide (rGO) [1, 11]. Such founding may open up the possibilities for cPDA to be used in various electronic applications, such as sensors, flexible electrodes, and protective shielding coatings.

However, the mechanical behavior of PDA and cPDA thin films, which is essential for design and fabrication of devices based on this material, is not well understood. Lin et al [12] has built in-silico models to simulate the mechanical properties of PDA with different crosslinking schemes. The results from simulation showed the Young's modulus of covalently linked PDA range from 4.1 GPa to 4.4 GPa. This result also matched the lower bound of their experimental results obtained from nanoindentation, which ranged from 4.3 GPa to 10.5 GPa. Lin also mentioned the heterogeneous nature of the PDA coating thickness and concluded this as the reason of large variation of the experimental results. It is important to point out that Lin and coworkers found the Young's modulus increased as the indentation penetration increased, which is an indication of substrate (silicon) effect. The lowest Young's modulus of 4.3 GPa corresponded to the smallest penetration of 150 nm. However, the authors did not provide detailed information about the thickness of the PDA thin films [12, 13]. Another study performed by Klosterman and coworkers tested PDA thin films using the buckling method. Results showed a Young's modulus of 2.0 GPa, which was lower than the in-silico model prediction (2.3 GPa). The authors argued that the simulation model only considered the internal forces within PDA granules, whereas inter-granular interaction would affect the experimental result. Therefore, inter-granular force is weaker than internal bonding [14].

While there exists some variation in the measurement data of PDA thin films [12, 14] the mechanical property of carbonized PDA has not been investigated. Furthermore, effect of other processing conditions, such as doping with metal ions, is unknown. The addition of metal ion dopant into polymer matrix incubates dative bonds with proper donor-acceptor combinations. With coordination bonds, the structure of the resultant often differs from its pristine form, so as the mechanical properties. Holten-Andersen et al. studied how the addition of metal ions or metal nanoparticles would affect hydrogels' mechanical properties by replacing intermolecular linkage from covalent bonding to coordination link [15]. In addition, the number of bonds formed between polymer and metal nanoparticles will also alter the property [16]. The mechanical property of hydrogel can also be tuned since the bonding is often chemically reversible [16].

This work aims to expend our knowledge on the mechanical behavior of PDA and its derived materials by studying the Young's modulus of PDA and Cu ion doped PDA as a function of heat treatment temperature. Nanoindentation was conducted on freestanding films, whose thickness was several times larger than the indentation penetration to minimize the substrate effect. Our results show both heat treatment and Cu doping led to increased Young's modulus.

EXPERIMENTAL DETAILS

Synthesis was conducted using a previously reported process [1, 2]. In brief, 2 mg/mL of dopamine hydrochloride powder (99%, Alfa Aeser, Haverhill, MA) was added into 50 mM tris buffer (pH = 8.5, Thermo Fisher Scientific Inc., Walthan, MA). For doping experiment, molar ratio of 1:1 was used between dopamine and $CuCl_2$ (Sigma-Aldrich, St. Louis, MO). The pH of the solution was adjusted back to 8.5 using 2M tirs buffer to ensure the alkaline environment for DA polymerization. Cleaned fused silica substrates were immersed in the solution. After 24 h, the substrates were removed, cleaned, and dried. Freestanding films floating on the solution surface were collected onto silicon substrates, and oven-dried. The dried films were heat treated in a tube furnace with running nitrogen at 300˚C and 600˚C. The nominal heating and cooling rate was fixed at 5˚C/min, a 60-min hold was performed at the peak temperature.

Nanoindentation was performed using a commercial unit (Triboindenter TI980, Bruker, Billerica, MA) with a conical tip under load control mode. The peak load was fixed at 25 μN. The loading, unloading segments were 2 sec, and the holding segment was 5 sec. Thickness of the thin films was measured using atom force microscopy (AFM, Bruker Demission Icon, Bruker, Billerica, MA). Surface morphology of the thin films was examined using scanning electron microscopy (SEM, FEI Quanta 450 FEG, FEI Inc. Hillsboro, OR) with a 10 kV acceleration voltage. TEM experiments (JEM 1400, JEOL, Tokyo, Japan) were conducted on powder samples suspended on copper TEM grids with carbon-formvar supporting film (Ted Pella Inc., Redding, CA). The acceleration voltage was fixed at 120 kV. Thermal stability of PDA and Cu-PDA powders was studied using differential scanning calorimetry (DSC 2500, TA Instrument, Inc, New Castle, DE) with a nominal heating and cooling rate of 10˚C/min.

RESULTS AND DISCUSSIONS

PDA coating on fused silica appeared to be brownish, which darkened with a blackish color after heat treatment at 600˚C (Figure 1(a)). This colour change is an indication of carbonization, which is accompanied by a mass loss and an increase in electrical conductivity [2]. Figure 1(b) shows an SEM image of a freestanding film collected on silicon substrate and oven dried in air. In contrast to crack-free PDA coatings on substrates [2], multiple cracks can be seen in the freestanding film. These cracks may be caused by the shrinkage of the PDA film during the drying process. After heat treatment, the roughness of freestanding film seemed to be reduced (Figure 1(c)) as the thickness decreased from ~ 570 nm prior to heat treatment to approximately 50 nm after heat-treated at 600˚C. In Figure 1(c), dark regions of cPDA were separated by cracks, which appeared bright due to electron charging. Our previous study showed the surface roughness within the uncracked regions was on the order of a few nanometers, which was not significantly affected by the heat treatment temperature [2].

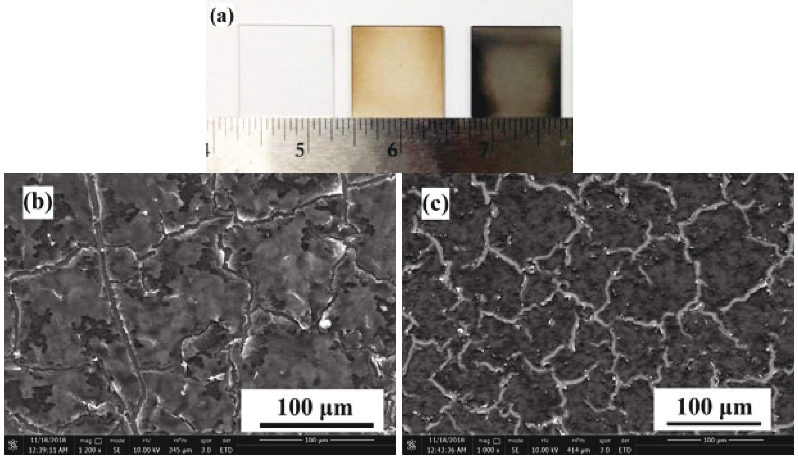

Figure 1: Images of PDA thin films. (a) Optical images of fused silica substrate (left), PDA coating on silica (middle), and carbonized PDA on silica substrate (right). (b) SEM image of PDA freestanding film collected on silicon substrate. (c) SEM image of PDA freestanding film after heat treatment at 300˚C.

Figure 2(a) shows a representative SEM image of Cu-ion doped PDA freestanding film. Cracks were still present. However, the Cu-PDA film seemed to be smoother without residual PDA particles (inset of Figure 2(a)). After heat treatment, nanoscale particles developed in the Cu-PDA thin film, accompanied by some surface roughening (Figures 2(b)&(c)). The surface roughening is related to the formation of Cu nanoparticles, which were approximately 0.9µm after heat treatment at 300°C (Figure 2(b)) and merge into bigger cluster as large as 3µm after heat treatment at 600°C (Figure 2(c). Figure 2(d) shows a TEM image of Cu-PDA powder after heat treatment. The dark circular dots were Cu nanoparticles, which were confirmed from electron diffraction analysis (Figure 2(e)). Therefore, it is believed that Cu ions initially doped into the PDA underwent a precipitation process to form metallic nanoparticles. The stability of Cu-PDA was also examined using differential scanning calorimetry (DSC), which showed an exothermic peak between 300˚C and 400˚C (Figure 3). This exothermic peak is likely related to the formation of Cu nanoparticles. In contrast, no such exothermic reaction was observed in pure PDA (Figure 3).

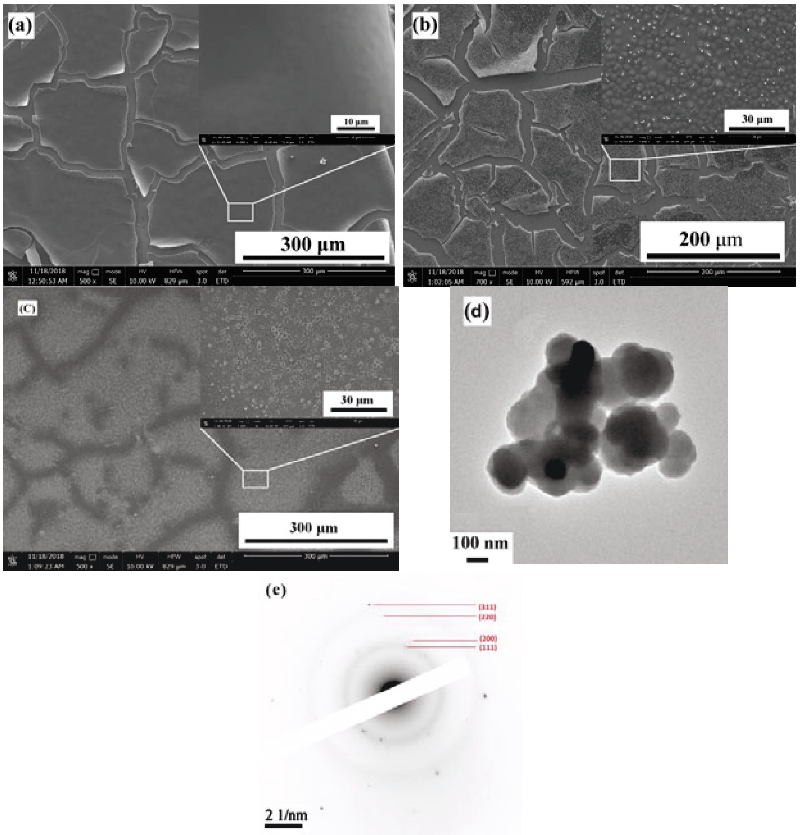

Figure 2: SEM images of freestanding Cu-PDA thin film collected on silicon substrate (a) before and (b) after heat treatment at 300˚C. (c) after heat treatment at 600 ˚C . (d)TEM image of Cu-PDA powder heat treated at 300˚C; and (e) selected area electron diffraction pattern of heat treated Cu-PDA powder.

To measure the mechanical properties, nanoindentation was performed on freestanding films. The film thickness varied from 50 nm and 570 nm (Table 1). At least 10 tests were conducted on each sample in the crack-free regions. The peak indentation depth varied between different materials. For PDA films without heat treatment, the indentation penetration was approximately 40 nm, which decreased to 10 nm in samples heat treated at 600˚C. Similar trend was observed on Cu-PDA films. For all samples, the indentation penetration was less than 1/5 of the total film thickness. Therefore, the substrate effect in this study is not significant.

The three curves included in Figure 4(a) showed very different behaviour, indicating the effect of heat treatment, thus the carbonization process, on the mechanical behaviour of PDA thin films. Under the same peak indentation load, the maximum indentation penetration decreased with increasing heat treatment temperature, implying increased stiffness. From the unloading portion of the curve, Young's modulus was calculated [17]. As shown in Figure 4(b), prior to heat treatment, PDA film had an average Young's modulus of 2.3 GPa, which is similar to the value reported by Klosterman et al [14]. After heat treatment, the Young's modulus increased to 7.2 GPa, which further increased to 14.7 GPa after heat treatment at 600˚C.

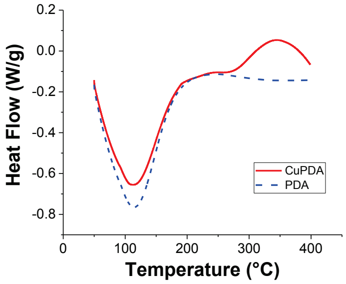

Figure 3: Heat flow during the heating of pristine and Cu doped PDA powders determined by differential scanning calorimetry.

Doping with Cu ion increased the Young's modulus of PDA. Without heat treatment, Cu-PDA film showed a Young's modulus of 10.2 GPa, which is more than three times higher than the pristine PDA film. It is possible that the Cu ions in the PDA promoted inter-granular interaction by introducing cross-linking bonds between PDA oligomers, which in turn enhanced the average bonding strength in PDA. Heat treatment also increased the Young's modulus of the Cu-PDA thin film. After heat treatment at 600˚C, the Cu-cPDA film exhibited a Young's modulus of 19.2 GPa (Figure 4(b)). This increase may be related to i) carbonization of the PDA phase, and ii) formation of Cu nanoparticles (Figure 2b).

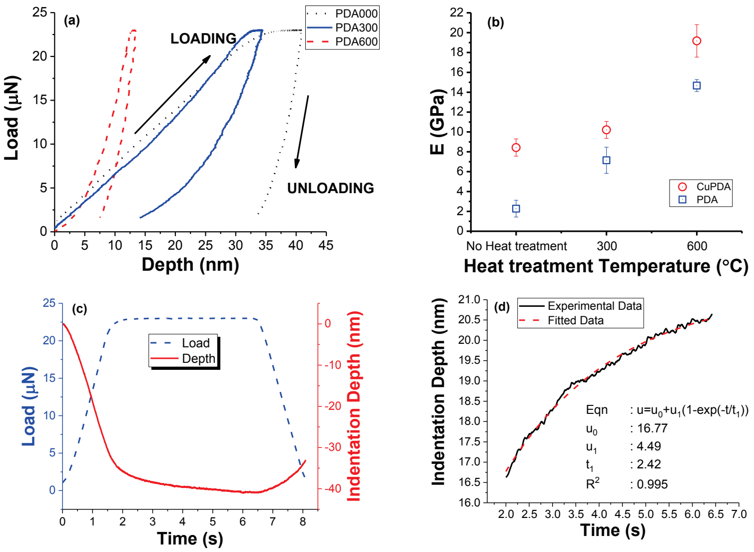

Figure 4: (a) Typical loading and unloading curve for PDA films with different treatment temperatures; (b) Young's modulus of pristine and Cu doped PDA film as a function of heat treatment temperature; (c) Typical time-dependent load and penetration curves during nanoindentation tests; (d) a selected curve showing time-dependent indentation depth during the hold period at peak load, and its fitting to the Generalized Kelvin model.

All samples exhibited some degree of creep (see plateaus in Figure 4(a)). This behavior is better illustrated in Figure 4(c), where when holding at the peak load (~ 2 to 5 sec), the indentation penetration depth continued to increase. The creep behavior observed during nanoindentation, indicating viscoelasticity in PDA materials, can be well described using a generalized Kelvin model [18]. As illustrated in Scheme 1, a Kelvin model consists of a spring element serially connected with several Kelvin units, which include a dashpot and a spring connected in parallel. In this work, the creep data, i.e. time-dependent indentation, can be well characterized by the simplest Kelvin model,

$$u = u_0 + u_1\left(1 - e^{-t/t_1}\right) \qquad (1)$$

where u is the indentation depth; t is the holding time; u_0, u_1, and t_1 are fitting parameters, which may be considered as the magnitude of instantaneous deformation, magnitude of time-dependent deformation, and relaxation time, respectively. An example of curve fitting to Equation (1) is shown in Figure 4(d). Fitting results of experimental data to the Kelvin model is listed in Table 1. The increase in heat treatment temperature, as well as the addition of Cu, seems to decrease the constant u_0 and u_1, which is consistent with the trend observed in Young's modulus (Figure 4(b)). Since u_0 represents the time-independent deformation and u_1 represents the time-dependent deformation, an increase in Young's modulus will result in decrease in both u_0 and u_1. For Cu-PDA samples, decreases in both u_1 and t_1 were observed with increasing temperature, implying the viscoelastic behavior was reduced in samples received heat treatment. However, the undoped PDA samples do not show a consistent trend in t_1, which deserves further investigation.

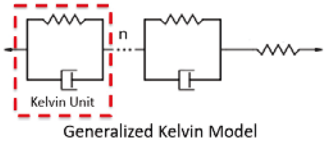

Scheme 1: Generalized Kelvin Model

Table 1: Average film thickness measured by AFM and fitting parameters to the general Kelvin creep model.

Sample	PDA	PDA300C	PDA600C	Cu-PDA	Cu-PDA300C	Cu-PDA600C
Thickness (nm)	570±26	276±48	65±9	512±23	393±37	55±9
u_0 (nm)	29.49±5.69	14.52±1.95	14.00±4.22	16.73±0.62	11.54±0.56	7.34±0.50
u_1 (nm)	4.54±0.42	1.18±0.24	0.81±0.13	3.74±0.56	0.89±0.26	0.43±0.03
t_1 (s)	2.02±0.35	4.92±0.46	2.60±1.67	2.43±0.25	2.18±0.41	0.50±0.11

CONCLUSIONS

In this work, mechanical properties of PDA and Cu ion doped PDA thin films were measured by nanoindentation technique. The Young's modulus of pristine PDA film without heat treatment was 2.3 ± 0.84 GPa. With heat treatment at 600˚C, this value increased to 14.7 ± 1.3 GPa. The addition of Cu ions in the PDA film increased the Young's modulus to 8.4 ± 0.9 GPa, which was further enhanced to 19.2 ± 1.6 GPa after heat treatment at 600˚C. Creep behavior was observed in both pure PDA and Cu-PDA, which can be described by a three-element generalized Kelvin model.

REFERENCES

1. H. Lee, S.M. Dellatore, W.M. Miller and P.B. Messersmith, *science* **318**, 5 (2007).
2. H. Li, Y.V. Aulin, L. Frazer, E. Borguet, R. Kakodkar, J. Feser, Y. Chen, K. An, D.A. Dikin and F. Ren. *ACS Appl Mater Interfaces* **9**, 6655 (2017).
3. X. Jiang, Y. Wang and M. Li, *Scientific Report* **4**, 4 (2014).
4. J.H. Ryu, P.B. Messersmith and H. Lee, *ACS Appl Mater Interfaces* **10**, 7523 (2018).
5. H. Li, T. Marshall, Y.V. Aulin, A.C. Thenuwara, Y. Zhao, E. Borguet, D.R. Strongin, F. Ren. *J. mater. Sci.* DOI:10.1007/s10853-019-03337-7 (2019).
6. D.R. Dreyer, D.J. Miller, B.D. Freeman, D.R. Paul and C.W. Bielawski, *Chem. Sci.* **4** (2013).
7. Y. Liu, K. Ai and L. Lu, *Chem Rev* **114**, 5057 (2014).
8. M.E. Lynge, R. van der Westen, A. Postma and B. Stadler, *Nanoscale* **3**, 13 (2011).
9. C.E. Brubaker and P.B. Messersmith, *Langmuir* **28**, 2200 (2012).
10. R. Li, K. Parvez, F. Hinkel, X. Feng and K. Mullen, *Angew Chem Int Ed Engl* **52**, 5535 (2013).
11. Z. Jia, P. Zhao, J. Ni, X. Shao, L. Zhao, B. Huang, B. Ge and C. Ban, *J. Mater. Eng. Preform.* **26**, 4434 (2017).
12. S. Lin, C.T. Chen, I. Bdikin, V. Ball, J. Gracio and M.J. Buehler, *Soft Matter* **10**, 457 (2014).
13. V. Ball, D.D. DFrari, M. Michel, M.J. Buchler, V. Toniazzo, Singh Manoj K., Gracio Jose and D. Ruch, *BioNanoScience* **2**, 18 (2011).

14. L. Klosterman, Z. Ahmad, V. Viswanathan and C.J. Bettinger, *Adv. Mater. Interfaces* **4**, 8 (2017).
15. N. Holten-Andersen, M.J. Harrington, H. Birkedal, B.P. Lee, P.B. Messersmith, K.Y. Lee and J.H. Waite, *Proc. Natl. Acad. Sci. U S A* **108**, 2651 (2011).
16. Q. Li, D.G. Barrett, P.B. Messersmith and N. Holten-Andersen, *ACS Nano* **10**, 1317 (2016).
17. W. Oliver and G. Pharr, *Journal of Materials Research* **7**, 19 (1992).
18. Q.V. Le, F. Meftah, Q.-C. He and Y. Le Pape, *Mechanics of time-dependent materials* **11**, 22 (2007).